LA-9137

UC-34
Issued: March 1982

LA--9137

DE82 013741

Two-Dimensional Radiation-Hydrodynamic Calculations for a Nominal 1-Mt Nuclear Explosion Near the Ground

Henry G. Horak
Eric M. Jones
Maxwell T. Sandford II
Rodney W. Whitaker
Richard C. Anderson
John W. Kodis

DISCLAIMER

DISTRIBUTION OF THIS DOCUMENT IS UNLIMITED

Los Alamos
Los Alamos National Laboratory
Los Alamos, New Mexico 87545

TWO DIMENSIONAL RADIATION-HYDRODYNAMIC CALCULATIONS FOR A NOMINAL 1-Mt NUCLEAR EXPLOSION NEAR THE GROUND

by

Henry G. Horak, Eric M. Jones, Maxwell T. Sandford II, Rodney W. Whitaker, Richard C. Anderson, and John W. Kodis

ABSTRACT

The two dimensional radiation-hydrodynamic code SN-YAQUI was used to calculate the evolution of a hypothetical nuclear fireball of 1-Mt yield at a burst altitude of 500 m. The ground-reflected shock wave interacts strongly with the fireball and induces the early formation of a rapidly rotating ring-shaped vortex. The hydrodynamic and radiation phenomena are discussed.

I. INTRODUCTION

In Ref. 1, J. Zinn describes the one-dimensional radiation hydrodynamic code RADFLO and presents an application of his method of calculating the evolution of a hypothetical 1-Mt yield nuclear fireball. Because two-dimensional effects become important when the fireball is close to the ground, we have extended his calculations into two dimensions by treating a 1-Mt burst at an altitude of 500 m. We applied the computer program SN-YAQUI, a variant of YOKIFER (described in Refs. 2, 3, and 4). SN-YAQUI was especially designed to be consistent with RADFLO, and the same 40 frequency groups, opacity, and equation of state tables for air used by Zinn are incorporated into this code.

SN-YAQUI is written in r-z cylindrical geometry and performs, in alternate steps, two main functions: (1) hydrodynamic evolution is followed in Lagrangian fashion with the code YAQUI (Ref. 5), and (2) radiative evolution is followed with a simplified version of the code TWOTRAN (Ref. 6), which is based on the method of discrete ordinates (or SN). Whenever necessary, an automatic particle-in-cell rezoning procedure[7] is carried out to prevent cell boundaries from becoming concave; temporary rezones also are performed regularly for the SN, which requires cells of rectangular cross section. Provision is made for the reflection of light from the ground surface in accordance with Lambert's law of diffuse reflection with a given albedo, to which a value of unity was assigned for the calculations reported here.

The initial conditions are obtained at an appropriate evolution time by adopting values of the physical parameters derived from RADFLO; the time chosen (0.1 s) is just before the shock strikes the ground. The initial physical quantities are specific internal energy (or temperature), density, and the radial and axial components of velocity (Figs. 1, 2, and 3). The values are interpolated from the RADFLO mesh containing ~100 spherical zones onto about half of the total 7000 (70 × 100) cells of the SN-YAQUI mesh. For the problem at hand, the length of a cell side averages ~10 m. In addition, a uniform distribution of some 250 massless marker particles is established within the fireball portion of the mesh (Fig. 4); these are moved with the instantaneous fluid velocities and serve as tracers for the debris material within the fireball. The values of the physical variables in ambient cells are set in accordance with a realistic model atmosphere consisting of the altitude profiles of pressure, temperature, density, and water vapor.

At certain preselected times, computer-derived graphs of the fireball are generated, showing the physical variables, isophotes, etc. In the following sections, we will discuss the shock wave, Mach stem, reflected shock/fireball interaction, rise and growth of the fireball, and radiation field.

II THE SHOCK WAVE AND MACH STEM

The primary shock wave originating from the detonation strikes the ground shortly after 0.1 s, reflects, and returns through the fireball (see Fig. 5). Compressive heating raises the sound speed behind the shock and the propagation speed of the reflected shock. Consequently, the Mach stem, the intersection surface of the two shocks, forms at the ground and with time increases vertically. Normally, the propagation of the Mach stem is complicated by the character of the terrain, by the ground shock, and sometimes by the presence of a near surface layer of heated air, which can cause a precursor shock to form. These effects are not included in this calculation, which considers an ideal ground surface. The reflected shock passes through the burst point at 0.24 s and merges completely with the primary shock at 1.0 s (Fig. 6). The calculated vertical distances of the primary and reflected shocks and the horizontal distance of the Mach stem from the sub detonation point are given as a function of time in Fig. 7a. The altitude of the triple point vs time is shown in Fig. 7b. Figure 8 gives the relative peak overpressure, $(p - p_0)/p_0$, where p is the peak pressure in the Mach stem and p_0 is the ambient pressure, and the relative peak dynamic pressure, $q/p_0 = 0.5 \rho v^2/p_0$, where ρ is density and v is velocity. A pressure cross section of the Mach stem at 0.63 s is shown in Fig. 9. The calculated Mach stem doesn't display the sharpness or high peak pressure that could be produced by finer zoning in the Mach stem region.

III. THE RING VORTEX, FLOW FIELD, AND FIREBALL RISE AND GROWTH

A "free-air" nuclear burst has negligible interaction between the fireball and reflected shock; however, buoyancy forces deform the rising fireball and eventually create a ring vortex (toroid). When the interaction occurs early, as in the present case, the strong reflected shock imparts high negative vorticity to the fireball similar to that produced by buoyancy (the upward velocities near the z axis are highest), and the ring vortex forms much earlier than it would from buoyancy alone. For a 1-Mt free air burst, the time of toroid formation is ~11 s, but for a burst altitude of 500 m, the calculated time is ~1.5 s. The following situation occurs (see Fig. 10): a center of negative vorticity forms behind the reflected shock and, at 0.20 s, has risen to an altitude of 70 m. By 0.375 s, it has migrated to 225 m; eventually it becomes the toroidal vortex. Figure 11a gives the altitudes of the vortex center and the fireball top and the horizontal radius of the fireball (1000 K isotherm) during the first 7 s. Figure 11b gives the horizontal and vertical coordinates of the vortex center for times to 70 s.

The flow field near the fireball displays a predictable, though dramatic, behavior. At first the velocities are directed radially outwards behind the primary shock. The reflected shock passes through mid fireball at 0.24 s with an accompanying updraft. The toroid is established by ~1.5 s; meanwhile, the primary shock and Mach stem continue to press outward, though ever weakening (the rezoning procedure eventually discards them from the mesh). The region immediately above the primary vortex and towards the z axis displays a strong positive vorticity (Fig. 10) that was originally created by an inward moving disturbance at ~0.13 s and is a manifestation of initial conditions obtained from RADFLO.

As the fireball rises, the updraft along the z axis continues and pulls in replacement air from several kilometers away. This creates the "afterwind" that is characteristically observed in low altitude explosions.[8] Velocity profiles along the z axis are shown in Fig. 12.

The marker particles revolve about the internal toroid axis (Fig. 13) with angular velocity during 1.5 to 9 s amounting to ~2 rad/s and linear speed ~240 m/s relative to the toroid, which in turn rises at ~80 m/s. By 20 s, the angular velocity of the toroid has decreased to ~10% of its initial value.

IV. RADIATION PHENOMENA

The calculated radiative evolution of the fireball is carried out with the method of discrete ordinates. At certain selected times, graphs are computer-generated to show isophotes and irradiances in several spectral bands for a given observer's position. For this purpose, it is most convenient and accurate to apply the method of characteristic rays; the emergent radiances of the fireball in the direction of the observer are obtained by the direct application of the formal solution to the equation of transfer. The details are given in Ref. 9.

Figure 14 shows the calculated emitted power of the fireball as a function of time summed over all wavelengths and in the red (λλ5600 to 6800 Å) and green (λλ4600 to 5600 Å) bands. These powers were computed by the SN method and are consistent with irradiances determined independently by integrating over radiances obtained from characteristic rays. The integral of radiated energy taken over the power time curve gives a "thermal fraction" of the total yield amounting to 29%.

Figure 15 shows calculated isophotes in the red wavelength band at selected times, as would be observed from a position located horizontally 500 km from the fireball. Table I gives the maximum temperature in the mesh and the maximum brightness temperature obtained from the isophotes in the visible spectral region for selected times. By 5 s, the fireball has developed a very prominent "skirt," which is the large, hot, but relatively quiescent, region beneath the rapidly rotating toroid. It arises as a consequence of the deformation of isotherms produced by the reflected shock (Fig. 16). Several calculated continuous spectra are shown in Fig. 17. Such spectra have rather coarse resolution amounting to ~500 Å at λ2600 Å, ~1000 Å in the visible, and ~2000 Å at ~1 μm.

TABLE I. Maximum Temperatures In Mesh And Maximum Brightness Temperature

Time (s)	T_{MAX} (K)	$T_{B,MAX}$ (visible) (K)
0.15	39000	
0.20	30000	3800
0.50	18000	7000
0.75	15000	7800
1.00	12500	7850
1.25	9600	
1.50	8300	
2.00	7100	6000
3.00	5800	4900
6.00	4800	3550
8.00	4500	3450
10.00	4100	3200

V. ACKNOWLEDGMENTS

We wish to thank J. Zinn for valuable discussions. A. Amsden, R. Gentry, and H. Ruppel assisted us with the YAQUI hydrodynamics, and W. Reed and K. Lathrop assisted in implementing a simplified version of the TWOTRAN radiation transport program.

REFERENCES

1. J. Zinn, "A Finite Difference Scheme for Time Dependent Spherical Radiation Hydrodynamics Problems," *J. Computational Phys.* 13, 569 (1973).

2. R. C. Anderson and M. T. Sandford II, "YOKIFER: A Two Dimensional Hydrodynamics and Radiation Transport Program," Los Alamos Scientific Laboratory report LA 5704 MS (January 1975).

3. M. T. Sandford II and R. C. Anderson, "Two Dimensional Implicit Radiation Hydrodynamics," *J. Computational Phys.* 13, 130 (1973).

4. M. T. Sandford II, R. C. Anderson, H. G. Horak, and J. W. Kodis, "Improved Implicit Radiation Hydrodynamics," *J. Computational Phys.* 19, 280 (1975).

5. A. A. Amsden and C. W. Hirt, "YAQUI: An Arbitrary Lagrangian Eulerian Computer Program for Fluid Flow at All Speeds," Los Alamos Scientific Laboratory report LA 5100 (March 1973).

6. K. D. Lathrop and F. W. Brinkley, "TWOTRAN II: An Interfaced, Exportable Version of the TWOTRAN Code for Two Dimensional Transport," Los Alamos Scientific Laboratory report LA 4848 MS (July 1973).

7. H. G. Horak, E. M. Jones, J. W. Kodis, and M. T. Sandford II, "An Algorithm for the Discrete Rezoning of Lagrangian Meshes," *J. Computational Phys* 26, 277 (1978).

8. S. Glasstone, Ed., *The Effects of Nuclear Weapons*, (US Atomic Energy Commission, Rev., 1962), pp. 33.

9. H. G. Horak and J. W. Kodis, "Slant Path Distances Through Cells in Cylindrical Geometry and the Computation of Isophotes," to be published as a Los Alamos National Laboratory LA series report.

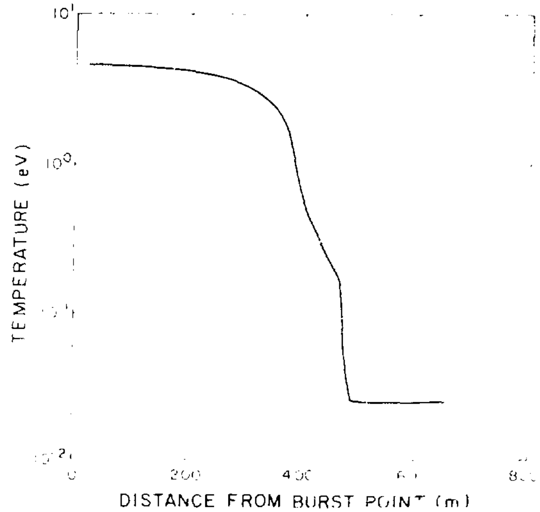

Fig. 1. Initial temperature distribution at 0.1 s.

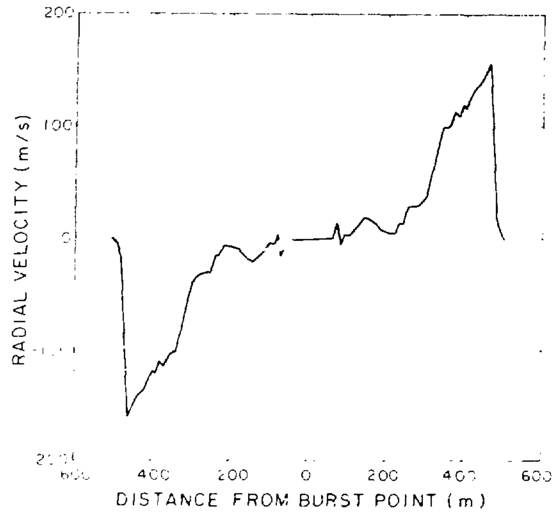

Fig. 3. Initial velocity distribution at 0.1 s.

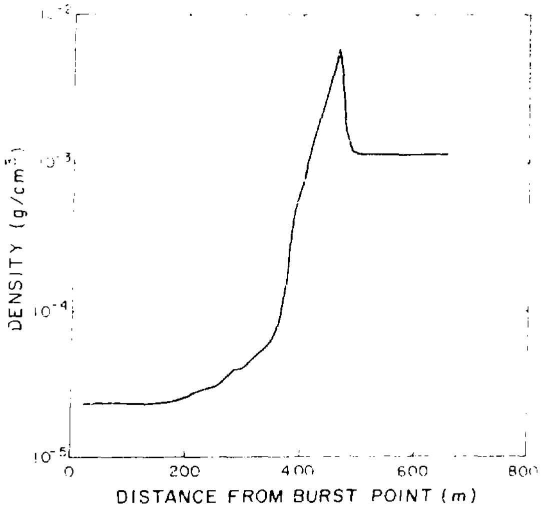

Fig. 2. Initial density distribution at 0.1 s.

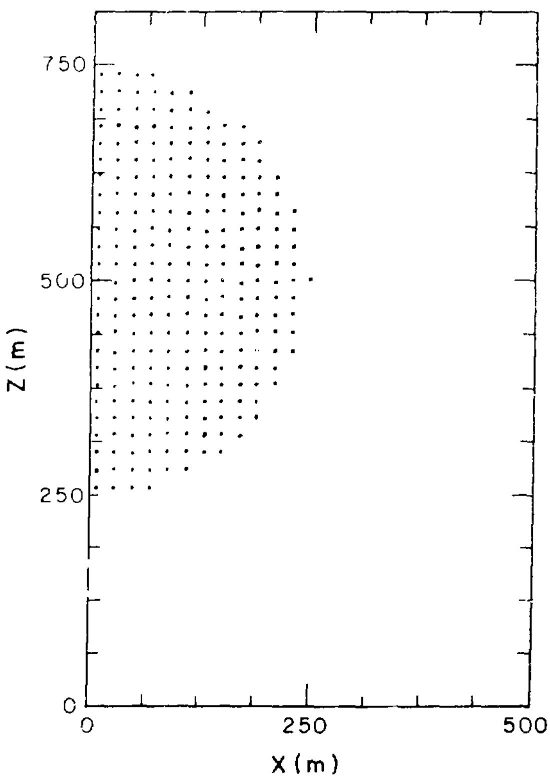

Fig. 4. Initial distribution of Lagrangian particles in the vertical plane x,z at 0.1 s.

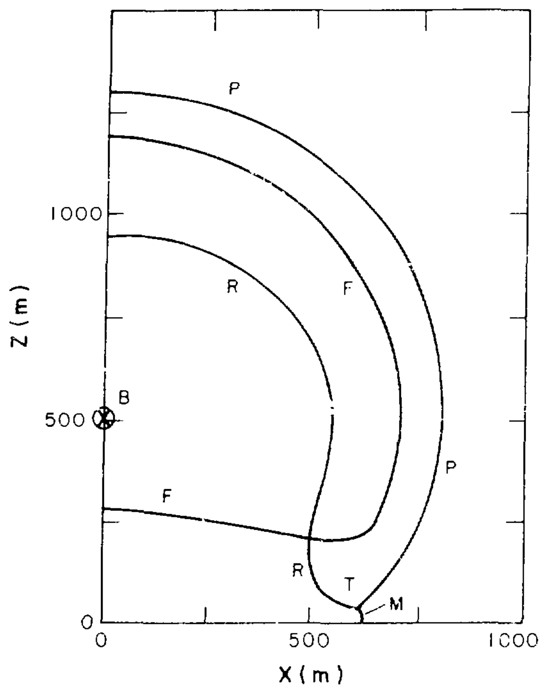

Fig. 5. A vertical cross section of the 1 Mt fireball at 0.5 s. B is the burst point, P is the primary shock, R is the reflected shock, M is the Mach stem, T is the triple point, and F is the 3000 K isotherm.

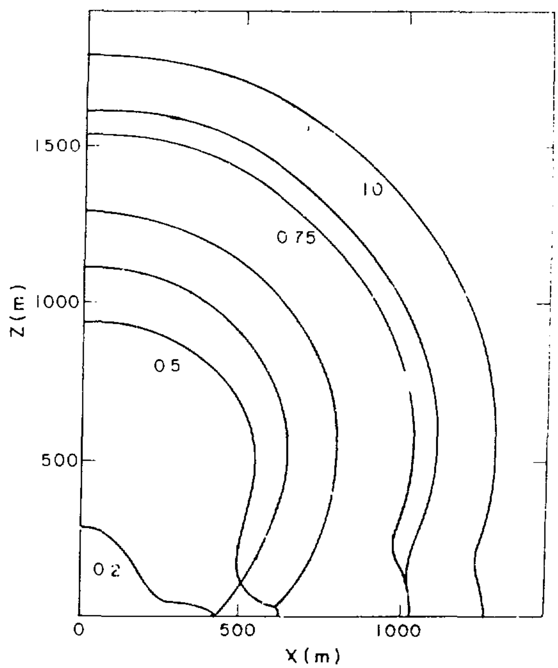

Fig. 6. The positions of the shocks in the vertical plane x,z at times 0.2, 0.5, 0.75, and 1.0 s.

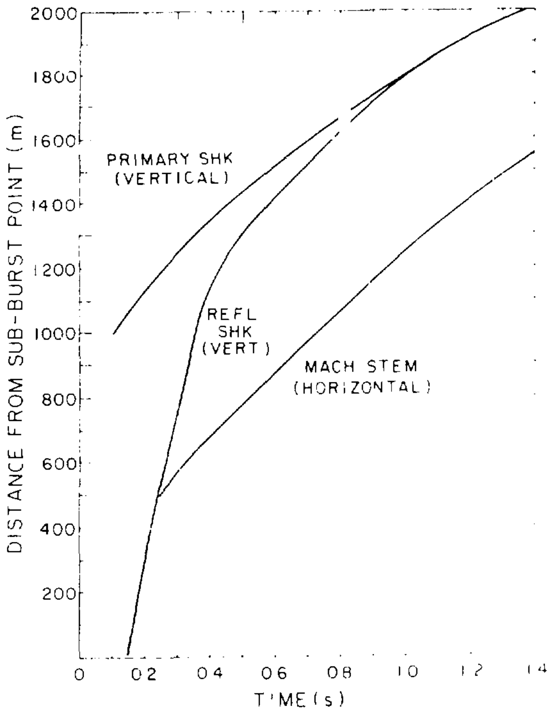

Fig. 7a. The vertical distances of the primary and reflected shocks and the horizontal distance of the Mach stem from the sub burst point as functions of time.

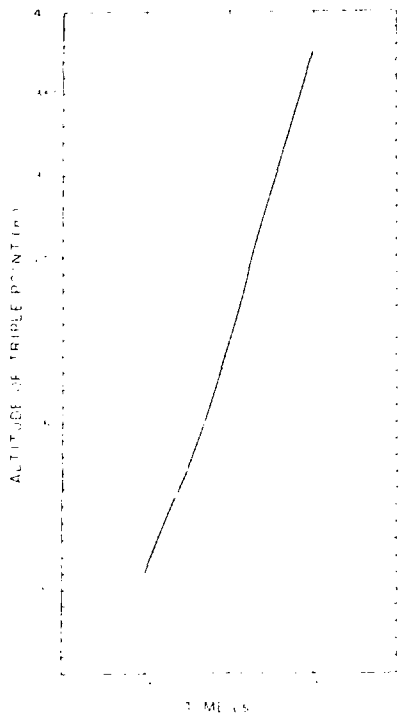

Fig. 7b. Altitude of the triple point vs time.

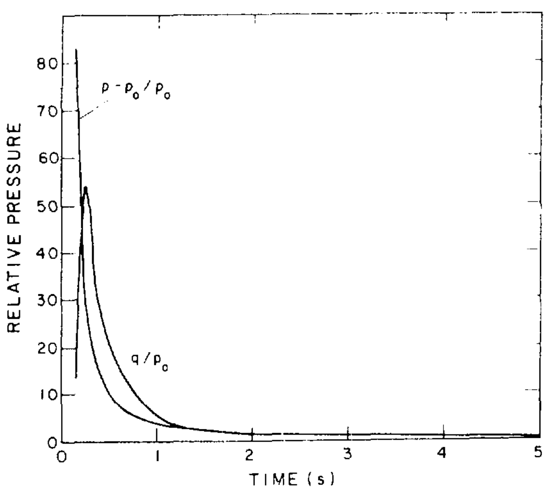

Fig. 8. The relative peak overpressure, $(p - p_o)/p_o$, and the relative peak dynamic pressure, q/p_o, in the Mach stem vs time.

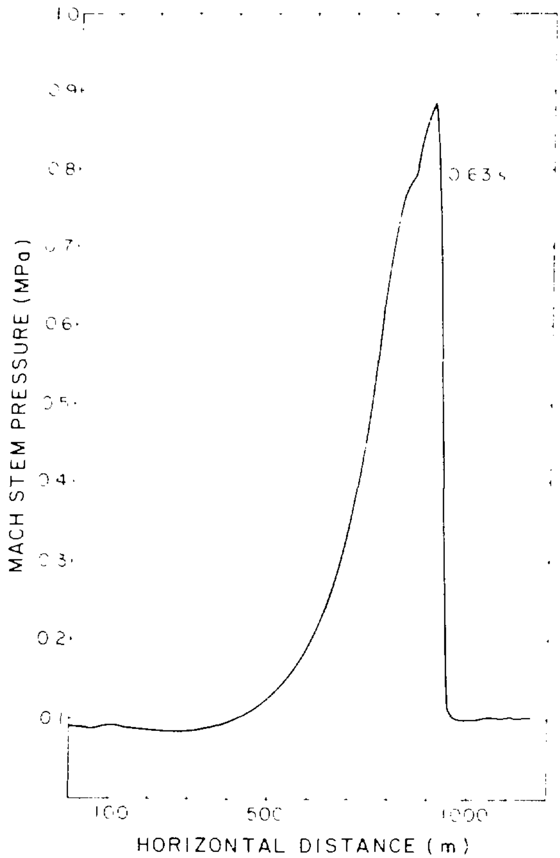

Fig. 9. The pressure profile through the Mach stem at ground level at 0.63 s.

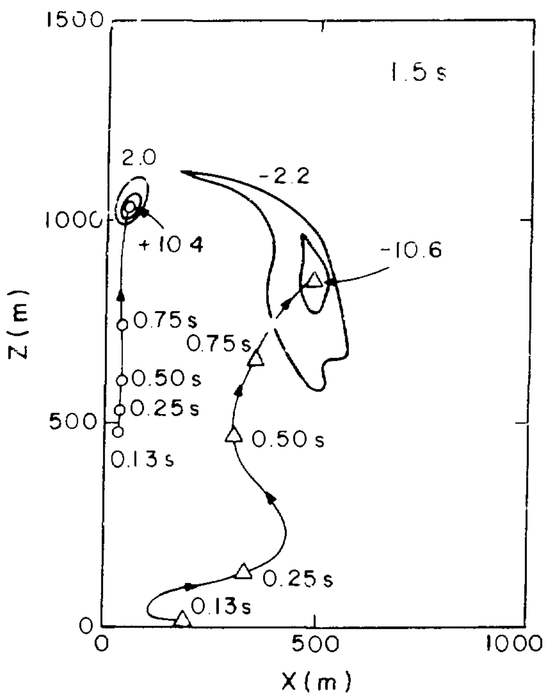

Fig. 10. A few isopleths of relative vorticity are shown at 1.5 s. Previous positions of the center of negative vorticity are indicated by △ and of positive vorticity by .

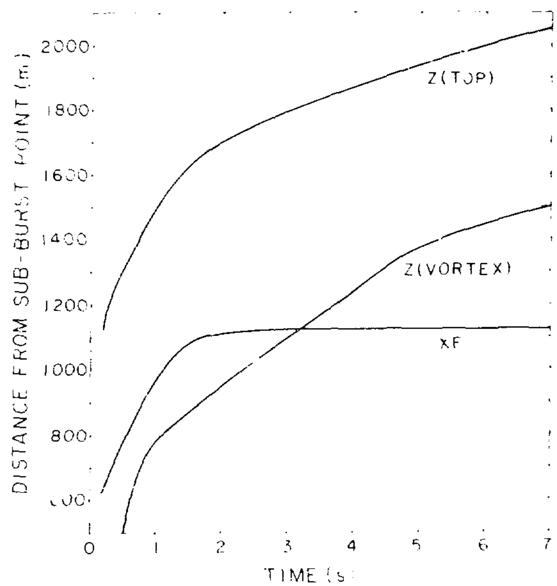

Fig. 11a. Z(TOP) is the altitude of the top of the fireball, and XF the horizontal radius of the fireball as defined by the 1000 K isotherm. Z(VORTEX) is the altitude of the center of the toroidal vortex.

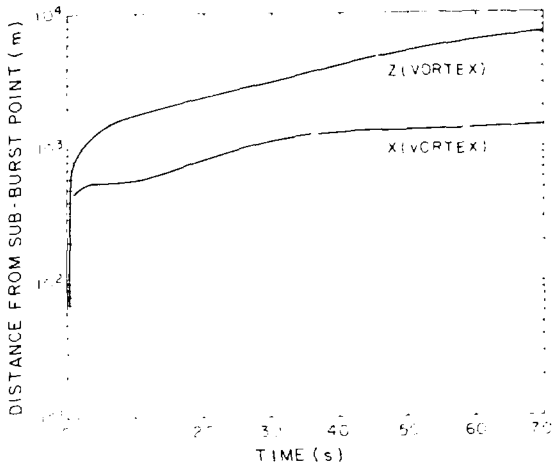

Fig. 11b. X(VORTEX) and Z(VORTEX) are the horizontal and vertical coordinates of the center of the toroidal vortex.

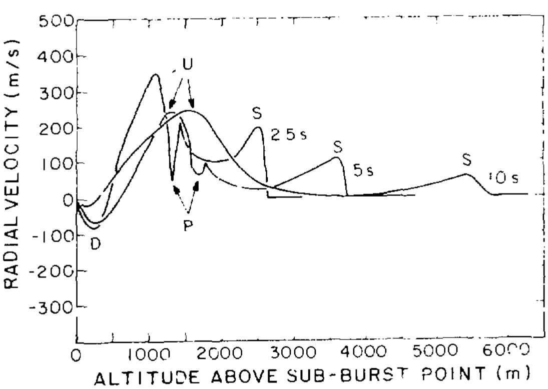

Fig. 12. Radial velocity curves along the z axis at 2.5, 5, and 10 s. The region of updraft is labeled U, downdraft D, shock S, and the small region of positive vorticity (Fig. 10) is labeled P.

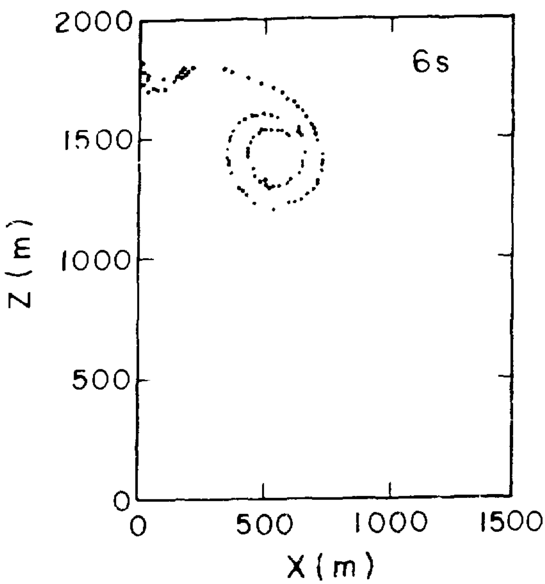

Fig. 13. Lagrangian marker particles at 6 s.

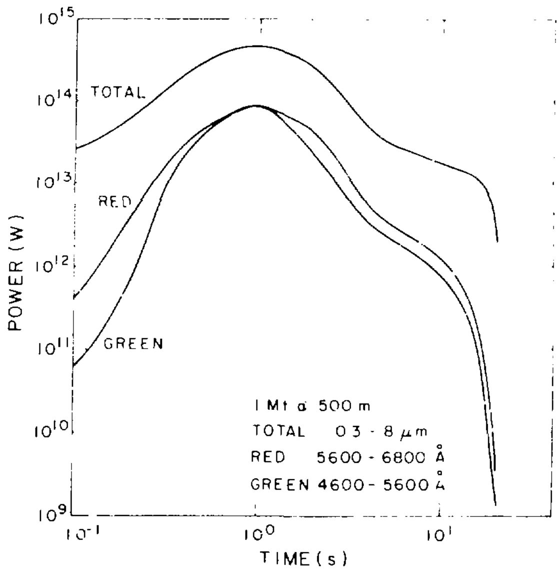

Fig. 14. Calculated emitted power of fireball as a function of time integrated over all bands (total) and for the red and green bands.

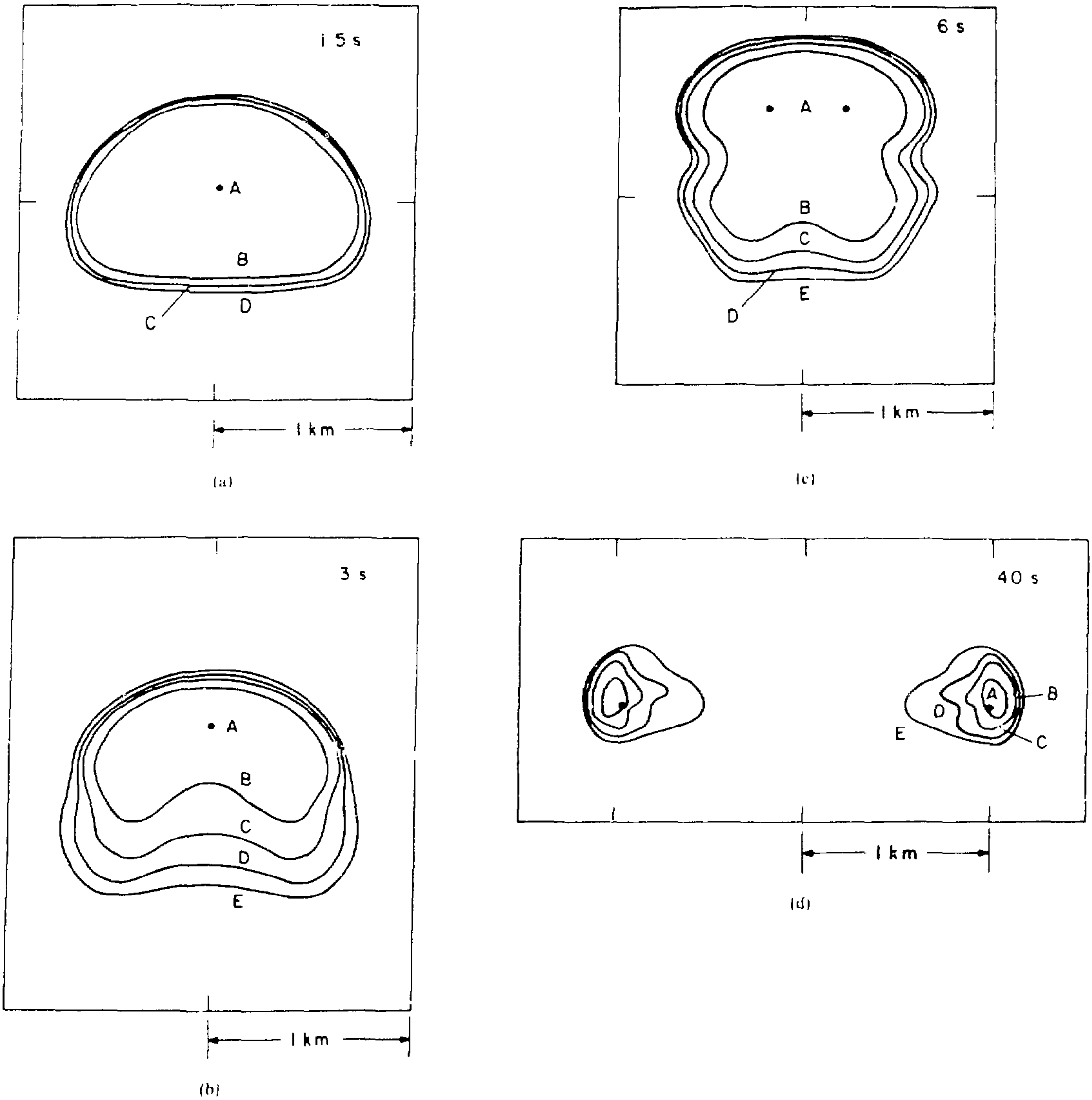

Fig. 15. Isophotes in the red band (5600 to 6800 Å) at selected times. The radiance factor between successive isophotes is 1.38. The brightest points are marked "A."

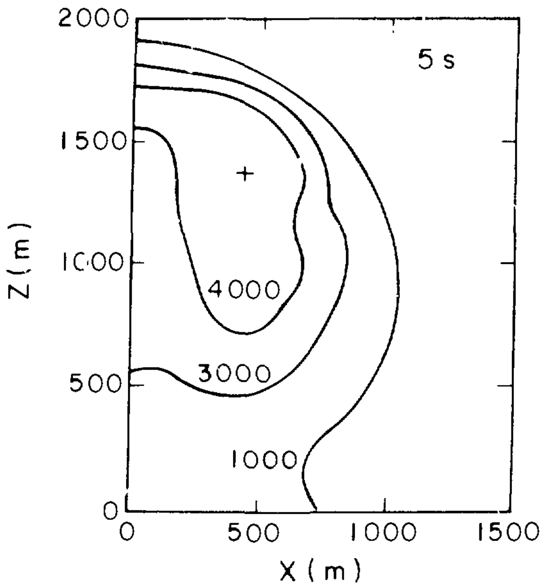

Fig. 16. Isotherms at 5 s. The center of the toroid is marked +.

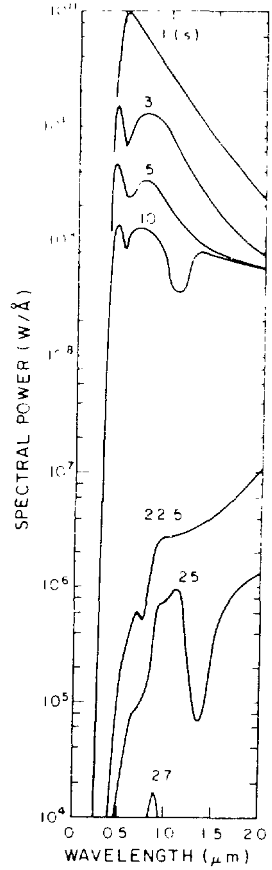

Fig. 17. Continuous spectra at various times.